

# Hyperfine structure of methanol lines at 25 GHz

J. S. Vorotyntseva<sup>1,2\*</sup> and S. A. Levshakov<sup>1,2†</sup>

<sup>1</sup>*Ioffe Physical-Technical Institute, Polytekhnicheskaya Str. 26,  
194021 St. Petersburg, Russia*

<sup>2</sup>*Department of Physics, Electrotechnical University “LETI”, Professor Popov  
Str. 5,  
197376 St. Petersburg, Russia*

## Abstract

High-dispersion (channel width  $\Delta_{\text{ch}} = 0.015 \text{ km s}^{-1}$ ) laboratory spectroscopy of the torsion-rotation lines  $J_2 \rightarrow J_1$  ( $J = 2 - 6$ ) in the ground torsional state ( $v_t = 0$ ) of the  $E$ -type methanol demonstrates multicomponent hyperfine splitting patterns at 25 GHz. The observed patterns are compared with simulations of  $\text{CH}_3\text{OH}$  emission lines based on *ab initio* quantum-mechanical models. A substantial disparity between the laboratory and simulated patterns is revealed. The observed morphology of the line shapes is not reproduced in the model profiles. The found inconsistency requires further refinement of the current quantum-mechanical models to fit the observed hyperfine splitting patterns at 25 GHz.

*Key words:* masers – methods: observational – techniques: spectroscopic – ISM: molecules – elementary particles.

## 1 Introduction

Radio astronomical observations of cosmic masers are widely used to investigate the physical conditions in star formation regions at different stages

---

\*E-mail: yuvorotynceva@yandex.ru

†E-mail: lev@astro.ioffe.ru

of evolution of protostellar objects and young stars. Of all known masers, methanol ( $\text{CH}_3\text{OH}$ ) is one of the most abundant tracers of dense and cold gas around protostars and in outflows (e.g., Leurini et al. 2007; Kalenskii & Kurtz 2016). Its abundance of  $10^{-9} - 10^{-7}$  (van der Tak et al. 2000) is high enough for methanol lines to be detectable in emission at different galactocentric distances up to the Galactic outskirts and in absorption at high redshifts.

Since frequencies of methanol transitions are very sensitive to the value of the electron-to-proton mass ratio,  $\mu = m_e/m_p$  (Jansen et al. 2011; Levshakov et al. 2011), this molecule is also one of the best probes of the hypothetical variability of  $\mu$  in space (Levshakov et al. 2022) and time (Muller et al. 2021).

The methanol lines at 25 GHz are closely spaced in frequency and can be observed simultaneously within the same frequency band at radio telescopes, thus minimizing systematic errors and allowing accurate measurements of relative radial velocities of different transitions. In addition, high-dispersion spectroscopy of these lines, available in laboratories, provides information on the hyperfine structure of the corresponding lines.

Furthermore, it was recently found that some of the methanol masers emit in a favorite hyperfine transition when only one of the hyperfine components is masing and forming the observed maser profile (Lankhaar et al. 2018; Levshakov et al. 2022).

The methanol  $\text{CH}_3\text{OH}$  is known to have a rich hyperfine spectrum. The nuclear spins of C, O, and H have the values  $I_{\text{C}} = 0$ ,  $I_{\text{O}} = 0$ , and  $I_{\text{H}} = 1/2$ , so that small line splittings of the order of 10 kHz are caused by nuclear magnetic dipole interactions such as spin-rotation, spin-torsion, and spin-spin. Such hyperfine structure, which looks like doublet, triplet, and quartet patterns in partly resolved profiles of the  $E$ - and  $A$ -type methanol transitions, was observed in high resolution spectra (Coudert et al. 2015; Belov et al. 2016; Xu et al. 2019). In particular, it was found that the velocity offset between the two main peaks,  $\Delta V_{\text{hyp}}$ , in the hyperfine splitting patterns, depends on the angular momentum  $J$ : for methanol  $E$  states, in the high frequency range of 100 – 500 GHz, the  $v_t = 0$  splittings *increasing* approximately as  $J$  for rotational quantum numbers  $J$  from 13 to 34 and  $K$  from  $-2$  to  $+3$  (Belov et al. 2016), but the  $v_t = 1$  splittings *decreasing* approximately as  $1/J$  for  $Q$  branch transitions with  $7 \leq J \leq 15$  and  $K' \leftarrow K'' = +6 \leftarrow +7$ ,  $3 \leq J \leq 18$  and  $K' \leftarrow K'' = +3 \leftarrow +2$ ,  $8 \leq J \leq 24$  and  $K' \leftarrow K'' = +8 \leftarrow +7$ ; and for  $P$  branch transitions with  $8 \leq J \leq 13$  and  $K' \leftarrow K'' = -2 \leftarrow -3$  (Xu et al. 2019).

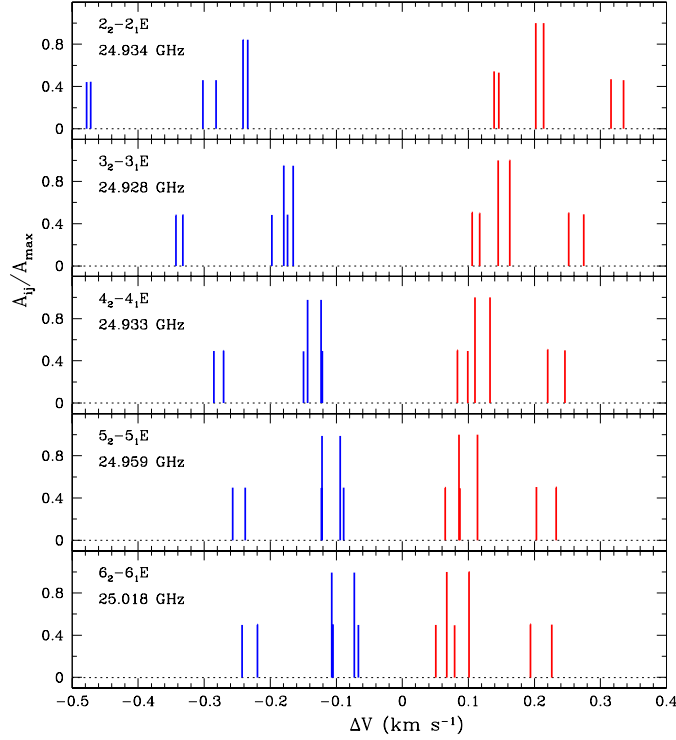


Figure 1: The hyperfine structure of the  $E$ -type methanol transitions  $J_2 \rightarrow J_1$  ( $J = 2 - 6$ ) in the ground torsional state ( $v_t = 0$ ) from Lankhaar (2022). The vertical bars show the strongest hyperfine components with a length proportional to their transition probability  $A_{ij}$  in units of the maximum Einstein coefficient  $A_{\max}$ . The zero velocity offset  $\Delta V$  corresponds to the transition central frequency which is indicated at the left top corner of each panel.

All of these facts make methanol a specific molecule for validating quantum-mechanical models of asymmetric-top molecules with hindered internal rotation.

The present short note deals with such tests based on our previous laboratory measurements in the low frequency range around 25 GHz in Hannover and Lille in 2012 (Coudert et al. 2015, hereinafter C15). To test quantum-mechanical models, accurate reconstruction of the hyperfine structure of the methanol lines is required. We re-processed our previous laboratory measurements at 25 GHz carried out in Hannover (C15) in order to improve the signal-to-noise ratio to a level which made it possible to deconvolve the line profiles into separate components.

## 2 Results

### 2.1 Model profiles

The detailed hyperfine structure of several torsion-rotational states of methanol was obtained by Lankhaar et al. (2016, hereinafter L16) from *ab initio* electronic structure methods and fits to experimental data of Heuvel & Dymanus (1973) and C15. Since that time, measurements of the hyperfine splittings of torsionally excited  $E$ -type methanol transitions in a high frequency range 100 – 500 GHz have been performed by Belov et al. (2016) and Xu et al. (2019), who derived their own fitting parameters of the effective Hamiltonian.

Note that the most comprehensive calculations of the spectroscopic properties of methanol are based on an extremely complex effective Hamiltonian containing a large number ( $> 100$ ) of fitting parameters (Xu & Hougen 1995; Xu et al. 2008). However, the successful use of such Hamiltonian, describing the global morphology of the observed methanol emission in a wide spectral range from microwave to infrared frequencies, does not guarantee an adequate description of the hyperfine structure of a particular methanol transition.

For instance, Lankhaar (2022, hereinafter L22) had to modify slightly the used in L16 effective Hamiltonian discarding some terms for the fitting formalism to align with Xu et al. (2019). The resulting hyperfine structure for several  $E$ -type torsion ground state transitions is shown in Fig. 1. In this figure, the vertical bars mark the strongest hyperfine components with a length proportional to their transition probability  $A_{ij}$  in units of the maximum Einstein coefficient  $A_{\max}$ . The velocity offsets,  $\Delta V$ , of the hyperfine subcomponents are given with respect to the transition central frequency which is indicated at the left top corner of each panel. The Doppler line broadening mechanisms leading to the overlap of individual hyperfine subcomponents will result in a multicomponent pattern which can be seen with a sufficiently high spectral resolution. Such patterns are displayed in Fig. 2 where the smooth blue and red curves represent the L16 and L22 models, respectively.

We note that the experimental spectrum of the  $4_2 \rightarrow 4_1E$  transition is asymmetric since the molecular signal (normally a symmetric doublet) will become asymmetric if the center frequency of the signal and the center frequency of the spectral mode of the Fabry-Pérot resonator do not coincide. This is not only due to the spectral envelope function of the resonator mode

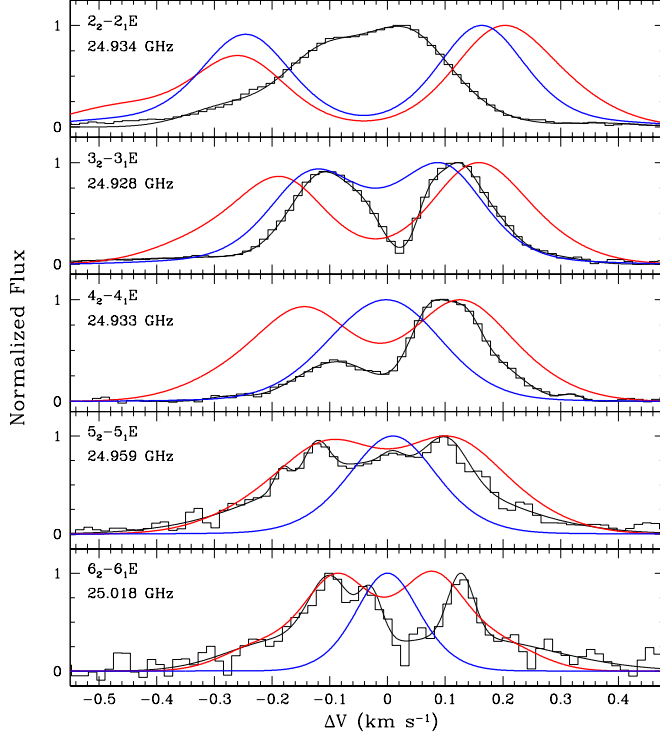


Figure 2: Comparison between observed and simulated hyperfine patterns for the  $J_2 \rightarrow J_1 E$  rotation-torsion transitions with  $J = 2-6$ . The black histograms display the observed hyperfine patterns recorded in Hannover (Coudert et al. 2015) and the superimposed black curves are their fits. The red curves represent convolutions of the overlapped hyperfine components which are illustrated schematically in Fig. 1 and based on quantum-mechanical calculations by Lankhaar (2022). The blue curves are the simulated profiles based on the earlier quantum-mechanical model by Lankhaar et al. (2016). In the experimental spectrum of the  $4_2 \rightarrow 4_1 E$  transition at  $\Delta V \approx -0.1 \text{ km s}^{-1}$  the lower amplitude of the doublet component as compared with the amplitude of the component at  $\Delta V \approx 0.1 \text{ km s}^{-1}$  is an artefact due to adjustments of the Fabry-Pérot resonator (for details, see Grabow 2004, 2011).

but also due to phase effects from the excitation as well as the emission of the molecular jet expanding along the resonator’s axis (for details, see Grabow 2004, 2011).

## 2.2 Laboratory profiles

The hyperfine splittings of about 10 kHz in case of the torsion-rotation lines  $J_2 \rightarrow J_1$  ( $J = 2 - 6$ ) in the  $E$ -type ground torsional state ( $v_t = 0$ ) of methanol at 25 GHz correspond to the velocity offsets of  $\Delta V_{\text{hyp}} \sim 0.12$  km s<sup>-1</sup>. Therefore, hyperfine components can be split at spectral resolution higher than this value. In the following we will use mainly our Hannover dataset at 25 GHz, but similar multicomponent hyperfine patterns were observed at different frequencies in Lille dataset (see, e.g., Fig. 1 in C15).

The experimental setup is described in detail in Sec. II of C15. We used the jet-based Fourier transform microwave spectrometer in high resolution mode with the channel width  $\Delta_{\text{ch}} = 0.015$  km s<sup>-1</sup>. It is worth noting that observed methanol emission lines were recorded as Doppler doublets, separated by the velocity interval  $\Delta V_{\text{dop}}$ , and that the line center of a given methanol transition was determined as the arithmetic mean of the peak frequencies of the two Doppler components. In due turn, each of the Doppler components displayed a multicomponent pattern with velocity separation between the main peaks of  $\Delta V_{\text{hyp}}$ . Of course, the  $\Delta V_{\text{hyp}}$  values are identical for the Doppler components of a given methanol transition. Therefore, to increase the signal-to-noise ratio ( $S/N$ ), we added both Doppler components together.

In Fig. 2 we compare laboratory profiles (shown by histograms) with the calculated hyperfine patterns based on quantum-mechanical models from L16 and L22 – blue and red curves, respectively. The physical parameters for the model profiles were chosen so that the full width at half maximum (FWHM) of the resulting profile of the convolved Gaussian profiles of the individual hyperfine transitions was approximately equal to the FWHM of the corresponding component of the laboratory profile. The model profiles were calculated under conditions of thermodynamical equilibrium. Each of the curves in Fig. 2 is normalized with respect to its peak intensity to facilitate comparison.

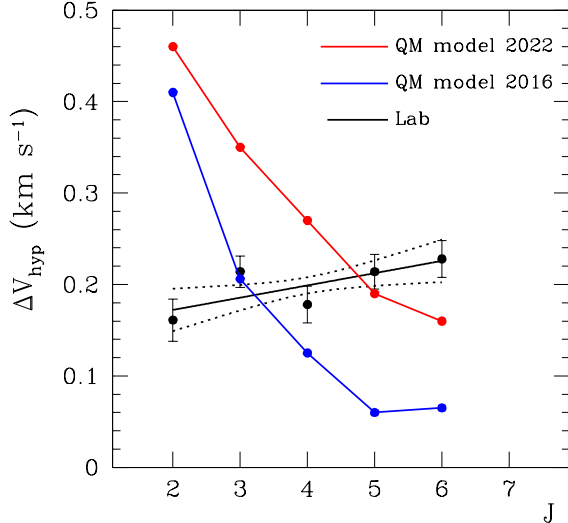


Figure 3: Comparison of the hyperfine splitting  $\Delta V_{\text{hyp}}$  as a function of the angular momentum  $J$  for different models with experimental data (dots with error bars). Shown are transitions  $J_2 \rightarrow J_1$  ( $J = 2 - 6$ ) of the  $E$ -type methanol at 25 GHz. The error bars of the laboratory measurements include statistical, model, and maximum systematic uncertainties (see text for details). The confidence zone for the regression line,  $\Delta V_{\text{hyp}}(J) = 0.0134(J - 4) + 0.199$ , is shown by the dotted lines.

### 2.3 Comparison of laboratory and model profiles

Visual inspection of Fig. 2 indicates a number of differences in the shapes of the profiles of methanol lines and in the magnitude of their splitting,  $\Delta V_{\text{hyp}}$ <sup>1</sup>. *First*, the gross structure of all lines in laboratory experiments is not traced by the model L16 except for the  $3_2 - 3_1 E$  line where one observes a closer qualitative consent to the experimental data. *Second*, the experimental multicomponent profiles of lines with  $J = 4 - 6$  are represented by a single and symmetric profile within the framework of the model L16. *Third*, although the model L22 shows better agreement with experiment, it does not reproduce morphology of lines with  $J = 5$  and 6.

We emphasize that both quantum-mechanical models L16 and L22 lead to the most significant discrepancies for the  $2_2 \rightarrow 2_1 E$  line – the line with almost merged two hyperfine peaks in the experimental data having the highest signal-to-noise ratio  $S/N \simeq 100$  in our Hannover dataset. Namely, both models give a broad pair of peaks in this case. It is also worth noting that the  $2_2 \rightarrow 2_1 E$  line lies outside the ascending frequency sequence with  $J$  changing from 2 to 17, and that it is located in this sequence between the

<sup>1</sup>We define the magnitude of the splitting as the velocity interval between peaks of maximum amplitude.

lines with  $J = 4$  and  $5$  (Müller et al. 2004).

The discrepancies in separations of the hyperfine components can be characterized quantitatively, comparing the values of the splitting  $\Delta V_{\text{hyp}}$ , which is shown in Fig. 3. Note that  $\Delta V_{\text{hyp}}$  for unsplit profiles with  $J \geq 4$  from the model L16 (shown by blue) are estimated from the calculated positions of the strongest hyperfine components. For the laboratory data, major errors are indicated, which include three sources of uncertainties: statistical, model, and systematic. The first is mainly due to the magnitude of the spectral channel  $\Delta_{\text{ch}}$  and the  $S/N$  ratio. The second is caused by ambiguity of the fitting procedure when, for instance, the  $5_2 \rightarrow 5_1 E$  and  $6_2 \rightarrow 6_1 E$  observed profiles can be fitted by models with different number of subcomponents. This leads to small changes in the  $\Delta V_{\text{hyp}}$  values. The third, the systematic uncertainty, is calculated from the Landé  $g$ -factors (Lankhaar et al. 2018) which were used in our estimations of the Zeeman offsets of the hyperfine lines at the maximum possible residual magnetic field ( $B \leq 1$  Gauss) in the spectrometer (C15).

As mentioned above, concordance between the simulated and laboratory  $\Delta V_{\text{hyp}}$  values is observed for the  $3_2 \rightarrow 3_1 E$  line from the model L16, and for the  $5_2 \rightarrow 5_1 E$  line from the model L22, but the latter has a different morphology.

The measured values of  $\Delta V_{\text{hyp}}$  are shown in Fig. 3 where we compare functional dependencies of  $\Delta V_{\text{hyp}}$  on  $J$  result from the experimental and model data. The quantum-mechanical values (red and blue points) have a tendency of decreasing the hyperfine splitting with increasing  $J$  in contrast to the laboratory measurements (black points with error bars) where one observes an opposite tendency. The experimental points were fitted to a straight-line model,  $\Delta V_{\text{hyp}}(J) = bJ + a$ , by the chi-square minimization method. The resulting linear regression line,  $\Delta V_{\text{hyp}}(J) = 0.0134(J - 4) + 0.199$ , shown by black in Fig. 3, provides  $\chi^2 = 4.065$  for  $\nu = 4$  degrees of freedom. This was our null hypothesis that  $\Delta V_{\text{hyp}}$  may be linearly dependent on  $J$ . The alternative hypothesis was that  $\Delta V_{\text{hyp}}$  is almost constant,  $\Delta V_{\text{hyp}} \approx 0.20 \text{ km s}^{-1}$  (17 kHz), for low frequency transitions at 25 GHz with  $J = 2 - 6$ . In this case  $\chi^2 = 7.265$  for  $\nu = 5$  degrees of freedom. In Fig. 3, we also show by two dotted lines the confidence zone for the null hypothesis at the significance level  $\alpha = 0.05$  following procedure from Bol'shev & Smirnov (1983).

The calculated regression line may be tested against the  $\chi^2$ -distribution with  $\nu = 4$  degrees of freedom. For this distribution, the critical value for the significance level  $\alpha = 0.05$  and  $\nu = 4$  is  $\chi^2 = 9.488$ , whereas  $\chi^2 = 11.070$  for



$\nu = 5$ . Since  $4.065 < 9.488$ , we cannot reject the null hypothesis. However, the alternative suggestion cannot be rejected as well, since  $7.265 < 11.070$ . In any case, we have no hard evidence that  $\Delta V_{\text{hyp}}$  is dependent on  $J$  for the transitions in question. New laboratory measurements with a high spectral resolution and a better  $S/N$  ratio would be desirable to check this statement for all  $J_2 - J_1E$  transitions with  $J = 2 - 17$  in the frequency range from 24.928 GHz to 30.308 GHz.

The discrepancies found and new laboratory experiments may help to constrain the structure of the effective Hamiltonian and spin-rotation operators in quantum-mechanical models of methanol to have better convergence between theory and experiment.

### 3 Summary

Refinement of quantum-mechanical models of the methanol molecule is important for the study of similar molecules with internal rotors detected in the interstellar medium (see, e.g., Table 1 in Kleiner 2019). The results obtained in this work show that the theoretical models do not exactly reflect laboratory observations – in most cases there are significant discrepancies in the magnitude of the hyperfine splittings and in morphology of the  $J_2 \rightarrow J_1E$  line profiles.

Nevertheless, the model L22 better describes the hyperfine structure of the observed line shapes than the model L16. The next step, therefore, is to refine the model L22 and to fit molecular constants and other torsion-rotation parameters.

## ACKNOWLEDGMENTS

The authors thank Boy Lankhaar for sharing with us his quantum-mechanical calculations of the methanol hyperfine structure and for valuable comments which stimulated this work. We also thank Jens-Uwe Grabow for details on adjustments of the Fabry-Pérot resonator. Our special thanks to an anonymous referee for diligent reading of our manuscript and useful remarks. Supported in part by the Russian Science Foundation under grant No. 23-22-00124.

## References

- Belov S. P., Golubiatnikov G. Yu., Lapinov A. V. et al. (2016) *J. Chem. Phys.* 145, 024307
- Bol'shev L. N., Smirnov N. V. (1983) *Tables of mathematical statistics* (Moscow, "Nauka")
- Coudert L. H., Guttlé C., Huet T. R., Grabow J.-U., Levshakov S. A. (2015) *J. Chem. Phys.* 143, 044304 [C15]
- Grabow J.-U. (2011) "Fourier Transform Microwave Spectroscopy Measurement and Instrumentation", *Handbook of High-Resolution Spectroscopy*, M. Quack and F. Merkt (eds.), John Wiley & Sons, Chichester, 723pp
- Grabow J.-U. (2004) "Chemische Bindung und interne Dynamik in großen isolierten Molekülen: Rotations-spektroskopische Untersuchung", *Habilitationsschrift*, Dem Fachbereich Chemie der Universität Hannover
- Heuvel J., Dymanus, A. (1973) *J. Mol. Spectrosc.* 47, 363
- Jansen P., Xu L.-H., Kleiner I., Ubachs W., Bethlem H. L. (2011) *Phys. Rev. Lett.* 106, 100801
- Kalenskii S., Kurtz S. (2016) *Astron. Reports* 60, 702
- Kleiner I. (2019) *ACS Earth Space Chem.* 3, 1812
- Lankhaar B. (2022) private communication [L22]
- Lankhaar B., Vlemmings W., Surcis G., et al. (2018) *Nat. Astron.* 2, 145
- Lankhaar B., Groenenboom G. C., Avoird van der A. (2016) *J. Chem. Phys.* 145, 244301 [L16]
- Laurini S., Schilke P., Wyrowski F., Menten K. M. (2007) *A&A* 466, 215
- Levshakov S. A., Kozlov M. G., Reimers D. (2011) *ApJ* 738, 26
- Levshakov S. A., Agafonova I. I., Henkel C. et al. (2022) *MNRAS* 511, 413
- Muller S., Ubachs W., Menten K. M., Henkel C., Kanekar N. (2021) *A&A* 652, A5
- Müller H. S. P., Menten K. M., Mäder H. (2004) *A&A* 428, 1019
- van der Tak F. F. S., van Dishoeck E. F., Caselli P. (2000) *A&A* 361, 327
- Xu L.-H., Hougen J. T., Golubiatnikov G. Yu. et al. (2019) *J. Mol. Spectros.* 357, 11
- Xu L.-H., Fisher J., Lees R. M. et al. (2008) *J. Mol. Spectros.* 251, 305
- Xu L.-H., Hougen J. T. (1995) *J. Mol. Spectros.* 173, 540